

Induced magnetism in superconductor using in a superconducting spin-valve

Hao Meng,^{1,2,3} Jiansheng Wu,^{1,*} Xiuqiang Wu,⁴ Mengyuan Ren,⁵ Yajie Ren,² and Jinbin Yao²

¹*Department of Physics, South University of Science and Technology of China, Shenzhen, 518055, China*

²*School of Physics and Telecommunication Engineering,*

Shaanxi University of Technology, Hanzhong 723001, China

³*Shanghai Key Laboratory of High Temperature Superconductors, Shanghai University, Shanghai 200444, China*

⁴*School of Mathematics and Physics, Yancheng Institute of Technology, Yancheng 224051, China*

⁵*College of materials science and engineering, Fuzhou University, Fuzhou 350116, China*

(Dated: November 17, 2016)

In general, it is considered that a noncollinear magnetization in superconductor (S) ferromagnet (F) heterostructure could create equal spin triplet superconducting correlations. It leads to the induced magnetic moment in the superconducting layer. In this paper, we demonstrate that in NSF_1F_2 spin-valve structure the induced magnetic moment emerging in S is provided by the conduction electrons forming spin singlet Cooper pairs (N : normal metal). This magnetic moment will penetrate from S into N , which can be attributed to the subgap in the N caused by the proximity effect. By tuning the exchange field and thickness of F_1 , the direction of the induced magnetic moment can be reversed due to the phase-shift acquired by the spin singlet pairs crossing the S/F_1 interface, but the variation of F_2 could not result in the same behavior. The above findings can explain previous and recent experiments [Stamopoulos *et al.*, Phys. Rev. B **72**, 212514 (2005); Flokstra *et al.*, Nat. Phys. **12**, 57 (2016); Ovsyannikov *et al.* J. Exp. Theor. Phys. **122**, 738 (2016)].

PACS numbers: 74.45.+c, 74.78.Fk

I. INTRODUCTION

The interplay between superconductivity and ferromagnetism in hybrid structures has currently attracted considerable attention because of the rich unusual physical phenomena¹⁻⁴ and potential practical applications⁵⁻⁹. Much effort has been devoted to obtaining a better understanding of these phenomena appeared in heterostructures involving superconductor (S) and ferromagnet (F). To mention a few of these, it is natural to highlight the experimental and theoretical study of the transport properties in SF structures.

It is well known that ferromagnetism and conventional superconductivity are two antagonistic orders, as ferromagnetism favors a parallel spin alignment, while Cooper pairs consist of electrons with antiparallel aligned spins. The interaction of superconductivity with ferromagnetism leads to suppression of the Cooper pairs in the ferromagnetic region. In this case, the spin-split of the electronic energy bands will make the Cooper pairs acquire a finite center-of-mass momentum $Q=2h_0/\hbar v_F$, where h_0 and v_F are the exchange field strength and the Fermi velocity, respectively. As a result, the Cooper pairs entering the ferromagnetic region become a mixture of singlet and triplet pairs $(|\uparrow\downarrow\rangle - |\downarrow\uparrow\rangle)\cos(QR) + i(|\uparrow\downarrow\rangle + |\downarrow\uparrow\rangle)\sin(QR)$, which rapidly decay in F as a function of the distance R from the S/F interface⁶⁻⁹. Another peculiarity in such systems is the spatial oscillations of these two components inside the F region⁶⁻⁹. Owing to this oscillatory nature, periodic π -phase shifts across the SFS junction will be displayed as a function of the thickness of the ferromagnetic layer¹¹. This will result in an oscillatory Josephson critical current, which has been confirmed by

the subsequent experiments¹²⁻¹⁵. By contrast, another unusual effect highlighted in the SF heterostructures is fact that a non-collinear magnetization in the ferromagnet may lead to the creation of spin-triplet superconducting correlations with equal spin projections $|\uparrow\uparrow\rangle$ or $|\downarrow\downarrow\rangle$ ⁸⁻¹⁰. These triplet components are not affected by the exchange field and can propagate long distance in ferromagnet and half-metal. Experimental evidence for this effect was reported in Refs.¹⁶⁻²⁰. Accordingly, this long-range proximity effect is prime examples of the potential that lies within this field of research.

While much of the work on SF proximity effect focused on the penetration of the superconducting order-parameter into the ferromagnet, very little was done to understand the penetration of ferromagnetic ordering into the superconductor. Originally, Bergeret *et al.*²¹ proposed that in the SF structure the magnetic moment may penetrate into the superconductor over the length scale of the superconducting coherence length ξ_S . This behavior could be understood physically by considering the contribution to the magnetization from Cooper pairs which were close to the S/F interface: the spin-up electron would prefer to be in the ferromagnetic region due to the exchange energy, while the spin-down electron remaining in the superconducting region then would give rise to a magnetization in the opposite direction of the proximity ferromagnet. This effect occurs only when the ferromagnetic layer is very thin or the exchange field is weak enough. Thereafter Kharitonov *et al.*²² showed theoretically that in the SF junction the induced magnetic moment in the superconductor displayed an oscillatory sign-changing behavior changing with the product h_0d of the exchange field h_0 and thickness d of the ferromag-

net. They thought that this surprising effect was due to peculiar periodic properties of localized Andreev states in the systems. In addition, the other groups also got the same theoretical results^{23,24}. Soon afterwards the manifestation of the magnetic moment penetrating into the superconductor was observed experimentally in the SF bilayers²⁵, perovskite SF multilayers²⁶, and FSF trilayers^{27,28}. Meanwhile, Löfwander *et al.*²⁹ presented theoretically that the spin-triplet superconducting correlations will lead to an induced spin magnetic moment in FSF trilayers with misalignment of the exchange fields in the two F layers. Recently, Pugach *et al.*³⁰ demonstrated that the superconducting triplet correlations should give rise to an induced magnetization in the Josephson junction with the composite non-collinear ferromagnetic interlayer. Such induced magnetization occurs at a relatively large distance and it is sensitive to the superconducting phase difference.

In addition, Stamopoulos *et al.*³¹ offered previously an interesting experimental result in the S /manganite multilayers/ F structures. They observed that the inhomogeneous magnetization structure of the manganite multilayers, which was modulated by the external magnetic field, could efficiently switch the direction of the magnetic moment appearing in the S region. Last year, Flokstra *et al.*³² found a very surprising effect in the NSF_1F_2 multilayered structure: the magnetic moment appears inside the normal metal layer, but not in the adjacent superconducting layer. In particular, the induced magnetic moment exhibits a spin-valve effect: a significant change in magnitude depends on the mutual orientation of magnetization in two ferromagnetic layer. Shortly afterwards, Ovsyannikov *et al.*³³ observed the magnetic moment induced into the superconducting part of the heterostructure that consists of a cuprate superconductor and a ferromagnetic spin valve when the magnetization vectors of the ferromagnetic films have noncollinear orientation. Nevertheless, a key issue still need to be resolved and further studied: which components, either the singlet or triplet pairs, could provide main contribution to the magnetic moment induced in the normal-metal and superconductor of the above three structures?

In this paper we present results for the induced magnetic moment in superconductor and corresponding changes in the NSF_1F_2 structure with arbitrary misalignment of the exchange fields in the two F layers. It is shown that by tuning the exchange field and thickness of the F_1 layer one may reverse the direction of the induced magnetic moment. In contrast, changing the characteristics of the F_2 layer the induced magnetic moment displays an oscillatory behavior but its direction can not be switched. If the exchange field of F_2 layer is strong enough, the oscillatory effect vanishes but the induced magnetic moment still exists in the S region. We consider that the above behavior is related to the long-range supercurrent through the system. The physical picture is that the singlet Cooper pairs could cross the S/F_1 interface and share their electrons between S layer and F_1

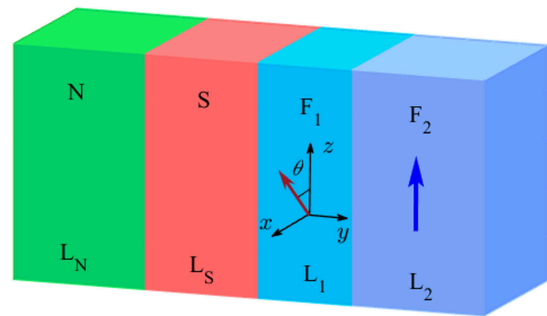


FIG. 1. (color online) Schematic of the NSF_1F_2 structure. Here the magnetization in F_1 layer can rotate in the x - z plane and its magnetization orientation is characterized by angle θ , whereas the magnetization of F_2 layer is fixed along the z direction. All layer widths are labeled.

layer, and then they can be converted to the equal spin triplet pairs in the F_2 layer. As a result, the conduction electrons of the singlet pairs could induce the magnetic moment in the S layer, and their phase-shift provided by the exchange field of the F_1 layer leads to the reversal of the induced magnetic moment. In contrast, the equal spin triplet pairs in the F_2 layer could not be affected by the exchange field of the F_2 layer. Accordingly, the variation of the F_2 layer could not reverse the direction of the induced magnetic moment. Moreover, a subgap will be produced in N region because of the proximity effect between S and N . So the N gets a small portion of superconductivity, and the induced magnetic moment will penetrate from the S layer into the N region.

II. MODEL AND FORMULA

The NSF_1F_2 junction we consider is shown schematically in Fig. 1. We denote the layer thicknesses by L_N , L_S , L_1 , and L_2 , respectively. The y axis is chosen to be perpendicular to the layer interfaces with the origin at the outer N surface. The exchange field \vec{h}_1 in the F_1 layer is tilted by angle θ from the z -axis in the x - z plane, while within the F_2 layer the exchange field \vec{h}_2 is directed along the z axis. We also assume that the whole system satisfies translational invariance in the x - z plane.

The BCS mean-field effective Hamiltonian^{6,34} is

$$H_{eff} = \int d\vec{r} \left\{ \sum_{\alpha} \psi_{\alpha}^{\dagger}(\vec{r}) H_e \psi_{\alpha}(\vec{r}) + \frac{1}{2} \left[\sum_{\alpha, \beta} (i\sigma_y)_{\alpha\beta} \Delta(\vec{r}) \psi_{\alpha}^{\dagger}(\vec{r}) \psi_{\beta}^{\dagger}(\vec{r}) + h.c. \right] - \sum_{\alpha, \beta} \psi_{\alpha}^{\dagger}(\vec{r}) (\vec{h} \cdot \vec{\sigma})_{\alpha\beta} \psi_{\beta}(\vec{r}) \right\}, \quad (1)$$

where $H_e = -\hbar^2 \nabla^2 / 2m - E_F$, $\psi_{\alpha}^{\dagger}(\vec{r})$ and $\psi_{\alpha}(\vec{r})$ represent creation and annihilation operators with spin α , and the vector $\vec{\sigma} = (\sigma_x, \sigma_y, \sigma_z)$ is composed of Pauli spin matrices. m is the effective mass of the quasiparticles in the system, and E_F is the Fermi energy. $\Delta(\vec{r})$ describes the

usual superconducting pair potential. The exchange field \vec{h} in the F region can be written as

$$\vec{h} = \begin{cases} h_1(\sin\theta\hat{x} + \cos\theta\hat{z}), & \text{in the } F_1 \text{ layer,} \\ h_2\hat{z}, & \text{in the } F_2 \text{ layer.} \end{cases}$$

Here \hat{x} (\hat{y}) is the unit vector along the x (y) direction.

In order to diagonalize the effective Hamiltonian, we make use of the Bogoliubov transformation $\psi_\alpha(\vec{r}) = \sum_n [u_{n\alpha}(y)\hat{\gamma}_n + v_{n\alpha}^*(y)\hat{\gamma}_n^\dagger]$ and take into account the anticommutation relations of the quasiparticle annihilation operator $\hat{\gamma}_n$ and creation operator $\hat{\gamma}_n^\dagger$. The resulting BdG equation can be expressed as³⁴

$$\begin{pmatrix} \hat{H}(y) & i\hat{\sigma}_y\Delta(y) \\ -i\hat{\sigma}_y\Delta^*(y) & -\hat{H}(y) \end{pmatrix} \begin{pmatrix} \hat{u}_n(y) \\ \hat{v}_n(y) \end{pmatrix} = E_n \begin{pmatrix} \hat{u}_n(y) \\ \hat{v}_n(y) \end{pmatrix}, \quad (2)$$

where $\hat{H}(y) = H_e\hat{\mathbf{1}} - h_z(y)\hat{\sigma}_z - h_x(y)\hat{\sigma}_x$ and $\hat{\mathbf{1}}$ is the unity matrix. Besides, $\hat{u}_n(y) = [u_{n\uparrow}(y), u_{n\downarrow}(y)]^T$ and $\hat{v}_n(y) = [v_{n\uparrow}(y), v_{n\downarrow}(y)]^T$ are quasiparticle and quasihole wave functions, respectively.

To acquire the local magnetic moment and the time dependent triplet amplitude functions, we solve the BdG equation (2) by Bogoliubov's self-consistent field method³⁴⁻³⁷. The NSF_1F_2 junction is placed in a one-dimensional square potential well with infinitely high walls, then the corresponding quasiparticle amplitudes can be expanded in terms of a set of basis vectors of the stationary states³⁸, $u_{n\alpha}(\vec{r}) = \sum_q u_{nq}^\alpha \zeta_q(y)$ and $v_{n\alpha}(\vec{r}) = \sum_q v_{nq}^\alpha \zeta_q(y)$ with $\zeta_q(y) = \sqrt{2/L} \sin(q\pi y/L)$. Here q is a positive integer and $L=L_N+L_S+L_1+L_2$. The pair potential in the BdG equation (2) satisfies the self-consistency condition³⁴

$$\begin{aligned} \Delta(y) &= \frac{g(y)}{2} \sum_n' \sum_{qq'} (u_{nq}^\uparrow v_{nq'}^{\downarrow*} - u_{nq}^{\downarrow} v_{nq'}^{\uparrow*}) \zeta_q(y) \zeta_{q'}(y) \\ &\times \tanh\left(\frac{E_n}{2k_B T}\right), \end{aligned} \quad (3)$$

where T is the temperature, and the superconducting coupling parameter $g(y)$ exists solely inside the superconducting region. The primed sum is over the eigenstates within range $|E_n| \leq \omega_D$, where ω_D is the Debye cutoff energy. The matrix elements of equation (2) are then written as

$$H_e(q, q') = \int_0^L \zeta_q(y) \left[-\frac{1}{2m} \frac{\partial^2}{\partial y^2} + \varepsilon_\perp - E_F \right] \zeta_{q'}(y) dy, \quad (4)$$

$$h_x(q, q') = h_1 \sin\theta \int_{L_N+L_S}^{L_N+L_S+L_1} \zeta_q(y) \zeta_{q'}(y) dy, \quad (5)$$

$$\begin{aligned} h_z(q, q') &= h_1 \cos\theta \int_{L_N+L_S}^{L_N+L_S+L_1} \zeta_q(y) \zeta_{q'}(y) dy \\ &+ h_2 \int_{L_N+L_S+L_1}^L \zeta_q(y) \zeta_{q'}(y) dy, \end{aligned} \quad (6)$$

$$\Delta(q, q') = \int_0^L \zeta_q(y) \Delta(y) \zeta_{q'}(y) dy, \quad (7)$$

where ε_\perp in equation (4) is the continuous energy in the transverse direction. The BdG equation (2) is solved by an iterative schedule. One first starts from the stepwise approximation for the pair potential and iterations are performed until the change in value obtained for $\Delta(y)$ does not exceed a small threshold value.

The local magnetic moment of the NSF_1F_2 geometry has two components³⁶,

$$\begin{aligned} M_x(y) &= -\mu_B \sum_n \sum_{qq'} [(u_{nq}^{\uparrow*} u_{nq'}^{\downarrow} + u_{nq}^{\downarrow*} u_{nq'}^{\uparrow}) f_n \\ &+ (v_{nq}^{\uparrow} v_{nq'}^{\downarrow*} + v_{nq}^{\downarrow} v_{nq'}^{\uparrow*})(1 - f_n)] \zeta_q(y) \zeta_{q'}(y), \end{aligned} \quad (8)$$

$$\begin{aligned} M_z(y) &= -\mu_B \sum_n \sum_{qq'} [(u_{nq}^{\uparrow*} u_{nq'}^{\uparrow} - u_{nq}^{\downarrow*} u_{nq'}^{\downarrow}) f_n \\ &+ (v_{nq}^{\uparrow} v_{nq'}^{\uparrow*} - v_{nq}^{\downarrow} v_{nq'}^{\downarrow*})(1 - f_n)] \zeta_q(y) \zeta_{q'}(y), \end{aligned} \quad (9)$$

where μ_B and f_n are the effective Bohr magneton and the Fermi function, respectively. It is convenient to normalize these two components to $-\mu_B$.

The amplitude functions of the spin triplet state with zero and net spin projection are defined, respectively, as follows³⁶

$$f_0(y, t) = \frac{1}{2} \sum_n \sum_{qq'} (u_{nq}^{\uparrow} v_{nq'}^{\downarrow*} + u_{nq}^{\downarrow} v_{nq'}^{\uparrow*}) \zeta_q(y) \zeta_{q'}(y) \eta_n(t), \quad (10)$$

$$f_1(y, t) = \frac{1}{2} \sum_n \sum_{qq'} (u_{nq}^{\uparrow} v_{nq'}^{\uparrow*} - u_{nq}^{\downarrow} v_{nq'}^{\downarrow*}) \zeta_q(y) \zeta_{q'}(y) \eta_n(t), \quad (11)$$

where the sum of E_n is in general performed over all positive energies, and $\eta_n(t) = \cos(E_n t) - i \sin(E_n t) \tanh(E_n/2k_B T)$. Additionally, the amplitude function of the spin singlet state can be written as $f_3 \equiv \Delta(y)/g(y)$. In this paper the singlet and triplet amplitude functions are all normalized to the value of the singlet pairing amplitude in a bulk superconducting material.

III. RESULTS AND DISCUSSIONS

Unless otherwise stated, the Fermi energy E_F is used as the unit of energy, and all lengths are measured in units of the inverse of the Fermi wave vector $k_F = \sqrt{2mE_F}/\hbar$. The normal-metal and superconductor thicknesses are set to fixed values $k_F L_N = 70$ and $k_F L_S = 50$, respectively. The Debye cutoff energy is taken as a fixed value $\omega_D/E_F = 0.1$.

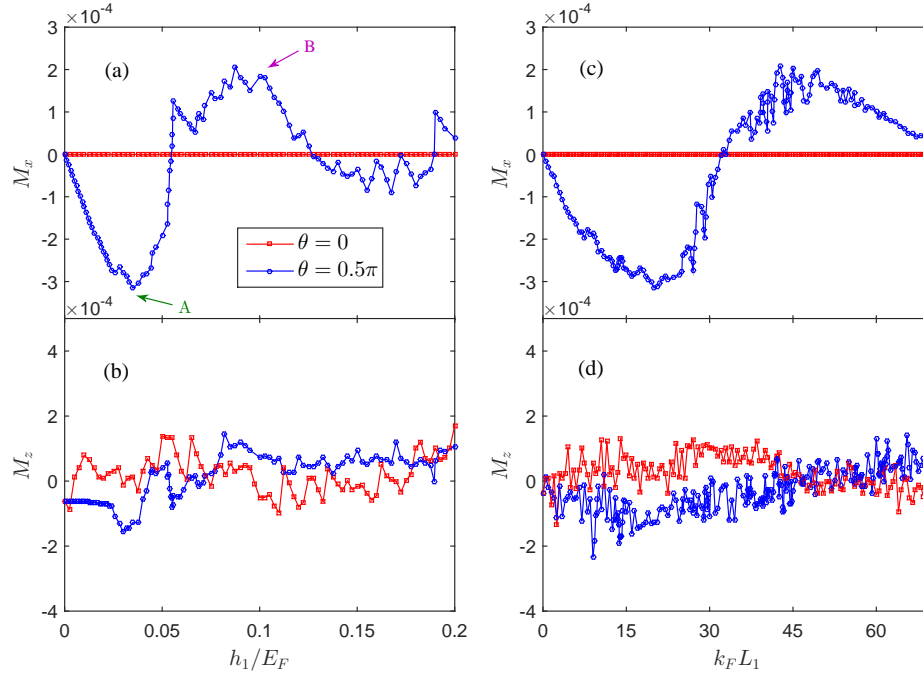


FIG. 2. (Color online) The induced magnetic moments M_x (a) and M_z (b) inside the superconducting region ($k_F y = 90$) as a function of exchange field h_1/E_F for thickness $k_F L_1 = 20$. The corresponding M_x (c) and M_z (d) as a function of thickness $k_F L_1$ for exchange field $h_1/E_F = 0.035$. All results shown in this figure are for $k_F L_2 = 50$, $h_2/E_F = 0.2$, and $k_B T = 0$. Two misorientation angles θ are considered as depicted in the legend.

In Fig. 2, we show the detailed dependence of the induced magnetic moments M_x and M_z inside the superconducting region on the exchange field h_1/E_F and thickness $k_F L_1$ for parallel and perpendicular orientations of the exchange fields. One can see that the magnetic moment M_x disappears completely for parallel orientation ($\theta = 0$). However, in the perpendicular case ($\theta = 0.5\pi$) the magnetic moment M_x is an oscillating sign-changing function of parameters h_1/E_F . This means that the direction of the magnetic moment M_x could be reversed by increasing the exchange field h_1/E_F . It is also found that in the above two cases M_z varies irregularly and its amplitude is usually much small. On the other hand, if one fixes the strength of exchange field h_1/E_F and changes the thickness $k_F L_1$, the induced magnetic moment could display the same behavior. Since the exchange field h_1/E_F is hardly variable in the experiment, one may hope to observe the oscillations of M_x performing measurements on samples with different thickness $k_F L_1$.

It would be interesting to find a physical argument for explaining the oscillations of the induced magnetic moment M_x . In the top panel of Fig. 3, we show the spatial profile of the induced magnetic moment M_x for two particular exchange fields $h_1/E_F = 0.035$ and 0.1 , which corresponds to the points A and B in Fig. 2 (a), respectively. In the former case, the induced magnetic moment M_x inside the S is negative and decays gradually as a function of distance from S/F_1 interface. Furthermore,

it is very interesting to observe that the induced moment M_x can penetrate from S into N . Its sign and magnitude almost remain unchanged in the N region. This phenomenon can be attributed to the proximity effect in the SN structure^{6,7}. In the case of S/N interface, the Cooper pairs can pass from the S to the N . Correspondingly, superconducting-like properties may be induced in the N , then a subgap will appear in this region. Therefore, the induced magnetization in the N has the same characters as the one in the S . The N region superconductivity obtained from the S layer could be demonstrated by spatial distribution of the singlet state, which is shown in the bottom panel of Fig. 3. The singlet states f_3 are able to penetrate over the entire N layer for two different exchange fields h_1/E_F because the width of N layer is thin enough. If one increases h_1/E_F the sign of M_x may turn from negative to positive, which can be attributed to the π phase-shift acquired by the singlet pairs. Detailed analysis will be described below.

We consider that the induced magnetic moment in the superconductor is closely related to the supercurrent passing through the junction. If the exchange field of the ferromagnet is weak or the ferromagnet shows an inhomogeneous magnetization, the supercurrent could pass through the whole system. In this case, the Cooper pairs composing the supercurrent could maintain a dynamic balance in the whole system, then it would form a special situation: the Cooper pairs share their electrons between both the superconductor and ferromagnetic layer.

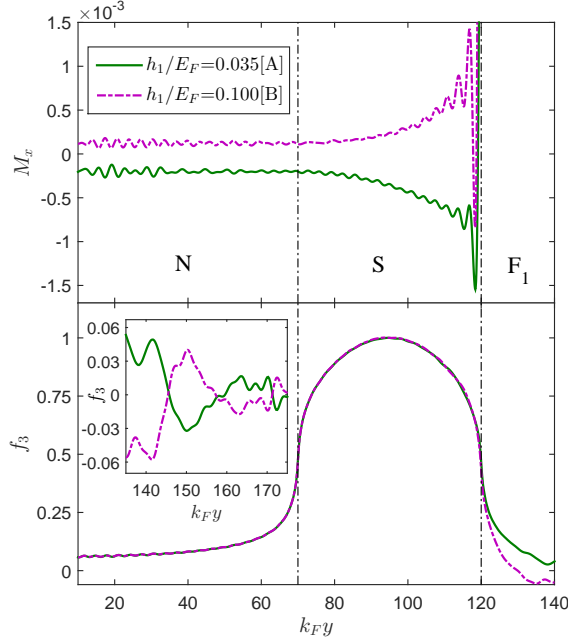


FIG. 3. (Color online) Spatial distribution of the induced magnetization M_x (top panel) and singlet state f_3 (bottom panel) for two particular exchange fields h_1/E_F in the perpendicular magnetic configuration ($\theta=0.5\pi$). The inset shows the detailed behavior of f_3 in the ferromagnetic region. The results plotted are for $k_F L_1=20$, $k_F L_2=50$, $h_2/E_F=0.2$, and $k_B T=0$. The vertical dash-dotted lines represent the location of the N/S and S/F_1 interfaces, respectively.

Let us first consider the parallel magnetization configuration. Because we have the direction of both ferromagnetic layers parallel to the z axis, the magnetic moment M_z will be induced in the superconductor when the exchange fields of the both ferromagnets are weak enough. The physical analysis is as follows²¹: in space near the S/F interface, since the two conduction electrons forming a Cooper pair are well spatially separated, the first of them may be hosted by the S while the second moves in the F . Undoubtedly, the spin of the second conduction electron should be aligned parallel to the ferromagnetic direction due to its interaction with the magnetization of the F . As a consequence the spin susceptibility of the first electron that reside in the S should be antiparallel to the one that is hosted in the F . Accordingly, the magnetic moment induced in the S is antiparallel to the magnetization direction of the F . However, if the exchange field or the thickness of the F is large enough, the supercurrent through system could be suppressed and therefore the above behavior of the Cooper pairs would never take place. As shown in Fig. 2 (b), the induced magnetic moment M_z shows a weak amplitude in the parallel configuration, which can be attributed to the suppression of the above Cooper pairs by the exchange field h_2/E_F . Meanwhile, the disappearance of the magnetic moment M_x in the parallel case could be ascribed to the nonexis-

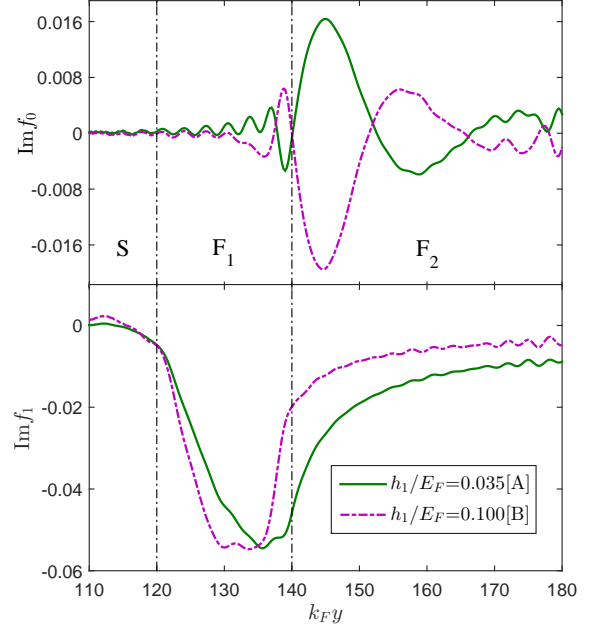


FIG. 4. (Color online) The spatial dependence of the imaginary parts of triplet components f_0 (top panel) and f_1 (bottom panel) for two exchange fields h_1/E_F . Other parameters are the same as in Fig. 3. The vertical dash-dotted lines represent the location of the S/F_1 and F_1/F_2 interfaces, respectively.

tence of x component of the magnetization in the F .

By contrast, since the magnetizations of both ferromagnets are perpendicular to each other ($\theta=0.5\pi$), the magnitude of M_z is still small enough, but the magnetic moment M_x becomes larger and also shows an oscillating sign-changing behavior with the increasing h_1/E_F . In this situation, the long-range supercurrent could pass through the entire system. The physical picture is summarized as follow: due to the exchange splitting of the energy bands in F_1 layer, the spin singlet state $|\uparrow\downarrow\rangle - |\downarrow\uparrow\rangle$ originating from the superconductor will acquire a center-of-mass momentum Q in the F_1 region, then this state can be transformed into $|\uparrow\downarrow\rangle_x e^{iQ \cdot R} - |\downarrow\uparrow\rangle_x e^{-iQ \cdot R}$, where R is the transmission distance from the S/F_1 interface. Accordingly, it can be rewritten as a mixture of the singlet component and the opposite-spin triplet component: $(|\uparrow\downarrow\rangle - |\downarrow\uparrow\rangle)_x \cos(QR) + i(|\uparrow\downarrow\rangle + |\downarrow\uparrow\rangle)_x \sin(QR)$. The singlet state is rotationally invariant, but the triplet state $(|\uparrow\downarrow\rangle + |\downarrow\uparrow\rangle)_x$ is equivalent to the equal spin triplet state $-(|\uparrow\uparrow\rangle - |\downarrow\downarrow\rangle)_z$ when viewed with respect to the z -axis, and that equal-spin state penetrates over a long distance in the F_2 layer^{8,9}. During the above research process, the F_1 layer magnetization along the x -axis is preferable to make the spin of one electron forming the singlet pair parallel to the same direction, then the spin of the other electron of the pair will be antiparallel to x -axis. As a result, the conduction electron inside the F_1 layer can be described as $|\uparrow\rangle_x e^{ik_{\uparrow} R}$. Correspondingly, in

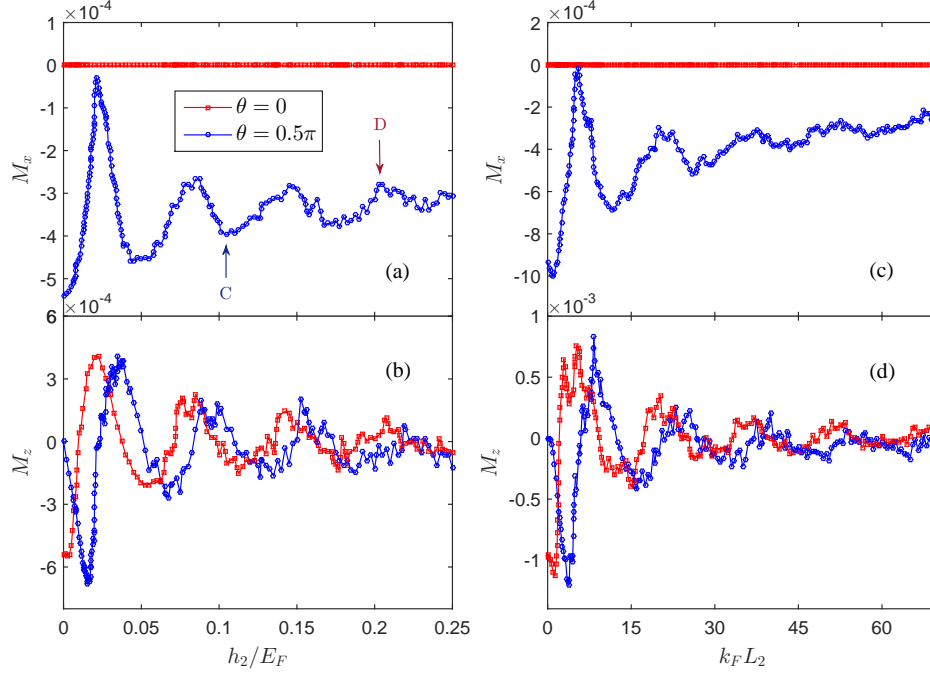


FIG. 5. (Color online) The induced magnetic moments M_x (a) and M_z (b) inside the superconducting region ($k_F y = 90$) as a function of thickness $k_F L_2$ for exchange field $h_2/E_F = 0.2$. The corresponding M_x (c) and M_z (d) as a function of exchange field h_2/E_F for thickness $k_F L_2 = 50$. All panels are plotted for $k_F L_1 = 20$, $h_1/E_F = 0.035$, and $k_B T = 0$.

the S region the other electron of pair is expressed as $|\downarrow\rangle_x e^{-ik_\perp R}$, where $k_{\uparrow(\downarrow)} = k_F + (-)Q/2$. Above two spin contributions to the pair amplitude are proportional to $e^{[\pm i(k_\uparrow - k_\downarrow)R]} = e^{\pm iQR}$. If the exchange field and thickness of F_1 layer are weak enough, the phase of the singlet and opposite-spin triplet components satisfies the condition $QR < \pi$. The direction of the magnetic moment in the superconductor is antiparallel to the F_1 layer magnetization. By contrast, if one makes the thickness $k_F L_1$ or the exchange field h_1/E_F grow big enough, the additional phase acquired by the pairs could fulfill the condition $QR > \pi$. In this case, the Cooper pair will acquire an additional π phase-shift, and the conduction electrons on both side of the S/F_1 interface will get a negative sign at the same time. Accordingly, the magnetic moment in the superconductor will be reversed. Our theoretical proposals may explain the experimental findings in Ref.³¹. In S /manganite multilayers/ F hybrid struture, the manganite multilayers including 15 bilayers $[\text{La}_{0.33}\text{Ca}_{0.67}\text{MnO}_3/\text{La}_{0.60}\text{Ca}_{0.40}\text{MnO}_3]_{15}$ could offer noncollinear magnetization. Because the thickness of the manganite multilayers is about 120 nm and the total effective exchange field is strong enough, the magnetic properties satisfy the condition $QR > \pi$. Since the external magnetic field is below the coercive field of the manganite multilayers, the magnetic moment of S should be parallel to the F layer magnetization. When the external field exceeds the coercive field the noncollinear magnetization will be reduced and it matches the condition

$QR < \pi$, then the S reverses its magnetization that could exhibit antiparallel feature.

The above physical analysis can be proved by the action of the singlet state f_3 and the triplet state f_0 in the ferromagnetic region. As shown in the bottom panel of Fig. 3, the singlet state f_3 could leak from S into F . For two different exchange fields $h_1/E_F = 0.035$ and 0.1 the both singlet states f_3 show antisymmetric structure in the F region, which indicates that the phase difference between them is π . Meanwhile, the two triplet states f_0 also show the same behavior (see the top panel of Fig. 4). In addition, we can see clear that the absolute value of M_x for $h_1/E_F = 0.1$ is smaller than that for $h_1/E_F = 0.035$. The reason can be attribute to the different magnitudes of the equal spin triplet state f_1 in the F_2 region, as illustrated in the bottom panel of Fig. 4. It is known that the decreasing of f_1 will reduce supercurrent through the whole system, and further affects the the number of conduction electrons crossing the S/F_1 interface. Eventually, it also leads to the decrease of the induced magnetic moment M_x in the superconductor. The detailed analysis of the modulation of the equal spin triplet state f_1 by the interface magnetization texture has been described in Ref.³⁹. Furthermore, it should be mentioned that the magnetic moment M_z will be induced in the superconductor in the case of the perpendicular magnetic configuration when the thicknesses and exchange fields of both ferromagnetic layers are all small. In such condition the singlet state f_3 could penetrate over the F_2 region, then

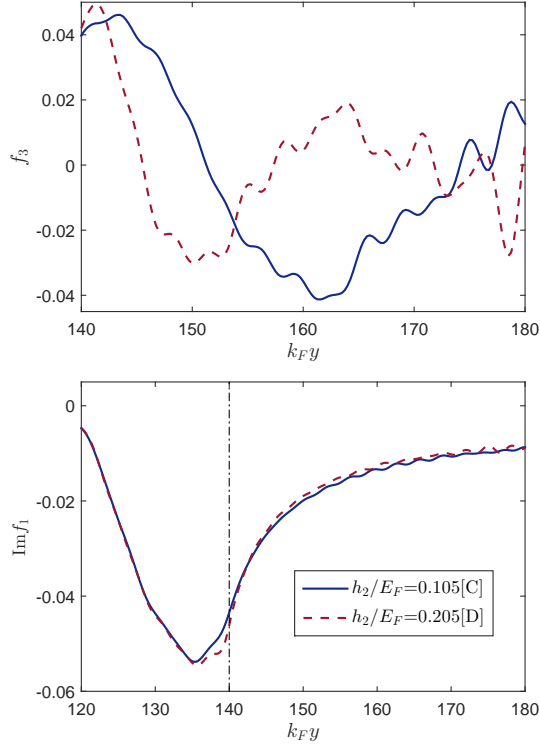


FIG. 6. (Color online) The spatial dependence of the singlet component f_3 (top panel) and the imaginary parts of triplet component f_1 (bottom panel) for two different exchange fields of F_2 layer. All panels are plotted for $k_F L_1=20$, $h_1/E_F=0.035$, $k_F L_2=50$, and $k_B T=0$. The vertical dash-dotted lines represent the location of the F_1/F_2 interface.

the singlet Cooper pairs share their electrons between the S and the F_2 layer. Therefore the S will acquire a magnetization component oriented along the z -axis. However, if the F_2 layer becomes a strongly spin-polarized ferromagnet, f_3 will be suppressed and then M_z decreases correspondingly.

Next, let us consider the dependence of the induced magnetic moments M_x and M_z on the characteristics of F_2 layer. From Figs. 5 (a) and 5 (b) we observe that in the parallel configuration ($\theta=0$) M_x disappears but M_z decays in an oscillatory manner with increasing exchange field h_2/E_F . In this case, the singlet Cooper pairs share their electrons between the S and the F_2 layer. Since the phase of the conduction electrons in the F_2 layer shifts with the exchange fields h_2/E_F , the phase of the other electrons inside the superconductor changes simultaneously. The phase-shift acquired by the conduction electrons will result in the sign change of M_z . Meanwhile, the singlet pairs could be suppressed by the exchange field h_2/E_F . This feature makes M_z decay with h_2/E_F . In particular, if h_2/E_F takes a larger value, M_z may be prohibited. On the other hand, for the perpendicular case ($\theta=0.5\pi$) the magnetic moment M_z presents the same oscillatory behavior. This

shows that the above-mentioned features of the singlet pairs are still valid in this case. However, the magnetic moment M_x always exhibits a negative value and also superimposes an oscillatory manner. This oscillation tends to decrease by increasing the exchange field h_2/E_F , and it would no longer exist for the large h_2/E_F . As described previously, the singlet state $|\uparrow\downarrow\rangle-|\downarrow\uparrow\rangle$ deriving from the S layer could be turned into a mixture state $(|\uparrow\downarrow\rangle-|\downarrow\uparrow\rangle)_x \cos(QR)+i(|\uparrow\downarrow\rangle+|\downarrow\uparrow\rangle)_x \sin(QR)$ in the F_1 layer. These two triplet states can produce different effect to the magnetic moment M_x . Firstly, the triplet state $(|\uparrow\downarrow\rangle+|\downarrow\uparrow\rangle)_x$ can be transformed to the triplet state $-(|\uparrow\uparrow\rangle-|\downarrow\downarrow\rangle)_z$ in the F_2 layer. These equal spin triplet pairs provide the main contribution to the transmission of long-range supercurrent and does not be affected by the the exchange field h_2/E_F . In this case, the number and phase of the original singlet pairs, which are converted into the equal spin triplet pairs, could not be changed by the exchange fields h_2/E_F . Accordingly, the direction of the magnetic moment M_x will remain unchanged. Secondly, the singlet state $(|\uparrow\downarrow\rangle-|\downarrow\uparrow\rangle)_x$ will transform into $(|\uparrow\downarrow\rangle-|\downarrow\uparrow\rangle)_z$ in the F_2 layer when the exchange field h_2/E_F is weak. This indicates that the singlet state is rotationally invariant during above rotating process. Thereupon the change of h_2/E_F will contribute an phase-shift to this fraction of singlet pairs, which leads to the amplitude oscillation of M_x . In order to analyse these characteristics we plot in Fig. 6 the spatial distributions of f_3 and the imaginary part of f_1 in the ferromagnetic region for $h_2/E_F=0.105$ and 0.205 , which correspond to two particular points C (valley value) and D (peak value) in Fig. 5 (a). It is found that both the singlet states f_3 clearly have π phase difference, but the two triplet states f_1 remain almost unchanged. So we can deduce that the oscillation of M_x is derived from the phase shift of f_3 obtained in the F_2 region, and the constant triplet state f_1 could make ensure that the sign of M_x is always negative. These numerical results are consistent with our previous analysis.

The dependence of the magnetic moment M_x on the misorientation angle θ and the temperature $k_B T$ are presented in Figs. 7 (a) and 7 (b), respectively. It is possible to find that the exchange field switching between parallel and orthogonal arrangements will lead to switching of M_x from zero to a negative value. This illustrates that M_x is proportional to the x component of magnetization in the F_1 layer. This effect may be used for engineering cryoelectronic devices manipulating the magnetic moment in the superconductor. Moreover, there is a large decrease in the magnitude of M_x as the temperature is enhanced. Specifically, if the temperature rises high enough M_x will disappear completely. This effect demonstrates that the induced magnetic moment is related to the singlet pairs crossing the S/F_1 interface but does not arise from the magnetization leakage from F_1 layer into S region.

Finally, we compare our theoretical result with the recent experiment investigated by Flokstra *et al*³². The primary difference between of them is that the induced

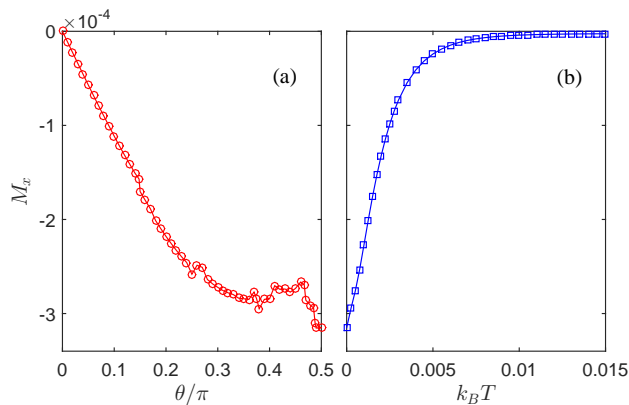


FIG. 7. (Color online) (a) The magnetic moment M_x plotted as a function of the misorientation angle θ for the case of zero temperature $k_B T = 0$. (b) The magnetic moment M_x as a function of the temperature $k_B T$ in the orthogonal arrangement ($\theta = 0.5\pi$). Parameters used in all panels are $k_F L_1 = 20$, $h_1/E_F = 0.035$, $k_F L_2 = 50$, and $h_2/E_F = 0.2$.

magnetic moment could generate in both S and N region for our result, but in the experiment of Ref.³² the induced magnetic moment appears not inside the S layer, and just exists in the adjacent N region. We envisage two kinds of speculations which could resolve the above contradictions. The first possibility is that the magnetic moment induced in the S is suppressed by other mechanisms, such as the spin-orbit interaction and orbital effects (Meissner currents)^{40,41}. The second one is that the induced magnetic moment itself exists in the superconductor, but the experiment did not observed it. From Fig. 2b in Ref.³² we can see that a part of the induced magnetic moment still exists in the superconductor although its amplitude is relatively small. Moreover, the magnetic moment induced in the superconductor has been demonstrated by the experimental observation³³. This further proves the correctness of our calculation result. On the other hand, we should point out that there are two same effects appearing in our result and the experiment observed by Flokstra *et al*³². (i) The induced magnetic moment in N region exhibits a spin-valve effect, which means the magnetic moment depends on the mutual orientation of the F layers' magnetization. (ii) The magnetic moment can be controlled by temperature. Below superconducting critical temperature T_c , appearance of the magnetic induction in the N layer is obtained for the orthogonal arrangement, but above T_c the corresponding magnetic moment does not exist.

IV. CONCLUSION

In this paper, we have investigated the magnetic moment induced in the superconductor by the electronic spin of the Cooper pair in clean NSF_1F_2S junctions with the misorientation magnetization. The long-range supercurrent through the system was pointed out as a source of this magnetic moment. We considered that the induced magnetic moment arises from the spin singlet pairs sharing their electrons between the S layer and the F_1 layer. The variation of the thickness and exchange field of the F_1 layer will lead to oscillatory sign-change behavior of the induced magnetic moment. This effect can be attributed to the phase-shift acquired by the singlet pairs in the F_1 layer. Moreover, the above singlet pairs can be converted into the equal-spin triplet pairs in the F_2 layer, which could not be affected by the exchange field of the F_2 layer. As a result, the induced magnetic moment maintains a constant sign if one changes the thickness and exchange field of the F_2 layer. In addition, the induced magnetic moment will increase with misorientation angle and reaches maximum for orthogonal arrangement, which can be used for engineering cryoelectronic devices manipulating magnetic moment in the superconductor. On the contrary, the induced magnetic moment will decrease with the enhancement of temperature. This demonstrates that the induced magnetic derives from the single pairs but not from the magnetization leakage from the F_1 layer into the S region. Beyond that, the induced magnetic moment can penetrate from the S into the N . This behavior can be attribute to the subgap appearing in the N region, which is caused by the proximity effect between the S and the N .

ACKNOWLEDGMENTS

This work was supported by the National Natural Science Foundation of China (Grants No.11447112, No.11604195, and No.11674152), Youth Hundred Talents Programme of Shaanxi Province, the Scientific Research Program Funded by Shaanxi Provincial Education Department (Grants No.15JK1132), the Opening Project of Shanghai Key Laboratory of High Temperature Superconductors (Grant No.14DZ2260700), and the Scientific Research Foundation of Shaanxi University of Technology (Grants No.SLG-KYQD2-01). J. Wu would like to thank the Shenzhen Peacock Plan and Shenzhen Fundamental Research Foundation (Grant No.JCYJ20150630145302225).

* wu.js@sustc.edu.cn

¹ Z. Nussinov, A. Shnirman, D. P. Arovas, A. V. Balatsky, and J. X. Zhu, Phys. Rev. B 71, 214520 (2005).

² I. B. Sperstad, J. Linder, and A. Sudbø, Phys. Rev. B 78, 104509 (2008).

³ M. Colci, K. Sun, N. Shah, S. Vishveshwara, and D. J. Van Harlingen, Phys. Rev. B 85, 180512(R) (2012).

- ⁴ K. Sun, N. Shah, and S. Vishveshwara, *Phys. Rev. B* 87, 054509 (2013).
- ⁵ A. A. Golubov, M. Yu. Kupriyanov, and E. Ilichev, *Rev. Mod. Phys.* 76, 411 (2004).
- ⁶ A. I. Buzdin, *Rev. Mod. Phys.* 77, 935 (2005).
- ⁷ F. S. Bergeret, A. F. Volkov, and K. B. Efetov, *Rev. Mod. Phys.* 77, 1321 (2005).
- ⁸ M. Eschrig, *Phys. Today* 64, No. 1, 43 (2011).
- ⁹ M. Eschrig, *Rep. Prog. Phys.* 78, 104501 (2015).
- ¹⁰ M. Eschrig and T. Löfwander, *Nature Phys.* 4, 138 (2008).
- ¹¹ F. S. Bergeret, A. F. Volkov, and K. B. Efetov, *Phys. Rev. B* 64, 134506 (2001).
- ¹² V. V. Ryazanov, V. A. Oboznov, A. Yu. Rusanov, A. V. Veretennikov, A. A. Golubov, and J. Aarts, *Phys. Rev. Lett.* 86, 2427 (2001).
- ¹³ T. Kontos, M. Aprili, J. Lesueur, and X. Grisson, *Phys. Rev. Lett.* 89, 137007 (2002).
- ¹⁴ Y. Blum, A. Tsukernik, M. Karpovski, and A. Palevski, *Phys. Rev. Lett.* 89, 187004 (2002).
- ¹⁵ J. W. A. Robinson, S. Piano, G. Burnell, C. Bell, and M. G. Blamire, *Phys. Rev. Lett.* 97, 177003 (2006).
- ¹⁶ Trupti S. Khaire, Mazin A. Khasawneh, W. P. Pratt, Jr., and Norman O. Birge, *Phys. Rev. Lett.* 104, 137002 (2010).
- ¹⁷ Carolin Klose, Trupti S. Khaire, Yixing Wang, W. P. Pratt, Jr., Norman O. Birge, B. J. McMorran, T. P. Ginley, J. A. Borchers, B. J. Kirby, B. B. Maranville, and J. Unguris, *Phys. Rev. Lett.* 108, 127002 (2012).
- ¹⁸ J. W. A. Robinson, J. D. S. Witt, and M. G. Blamire, *Science* 329, 59 (2010).
- ¹⁹ R. S. Keizer, S. T. B. Goennenwein, T. M. Klapwijk, G. Miao, G. Xiao, and A. Gupta, *Nature* 439, 825 (2006).
- ²⁰ M. S. Anwar, F. Czeschka, M. Hesselberth, M. Porcu, and J. Aarts, *Phys. Rev. B* 82, 100501 (2010).
- ²¹ F. S. Bergeret, A. F. Volkov, and K. B. Efetov, *Phys. Rev. B* 69, 174504 (2004); F. S. Bergeret, A. Levy Yeyati, and A. Martn-Rodero, *Phys. Rev. B* 72, 064524 (2005).
- ²² M. Yu. Kharitonov, A. F. Volkov, and K. B. Efetov, *Phys. Rev. B* 73, 054511 (2006).
- ²³ K. Halterman and O. T. Valls, *Phys. Rev. B* 69, 014517 (2004).
- ²⁴ J. Linder, T. Yokoyama, and A. Sudbo, *Phys. Rev. B* 79, 054523 (2009).
- ²⁵ Jing Xia, V. Shelukhin, M. Karpovski, A. Kapitulnik, and A. Palevski, *Phys. Rev. Lett.* 102, 087004 (2009).
- ²⁶ J. Stahn, J. Chakhalian, Ch. Niedermayer, J. Hoppler, T. Gutberlet, J. Voigt, F. Treubel, H-U. Habermeier, G. Cristiani, B. Keimer, and C. Bernhard, *Phys. Rev. B* 71, 140509(R) (2005).
- ²⁷ R. I. Salikhov, I. A. Garifullin, N. N. Garifyanov, L. R. Tagirov, K. Theis-Bröhl, K. Westerholt, and H. Zabel, *Phys. Rev. Lett.* 102, 087003 (2009).
- ²⁸ R. I. Salikhov, N. N. Garifyanov, I. A. Garifullin, L. R. Tagirov, K. Westerholt, and H. Zabel, *Phys. Rev. B* 80, 214523 (2009).
- ²⁹ Tomas Löfwander, Thierry Champel, Johannes Durst, and Matthias Eschrig, *Phys. Rev. Lett.* 95, 187003 (2005).
- ³⁰ N. G. Pugach and A. I. Buzdin, *Appl. Phys. Lett.* 101, 242602 (2012).
- ³¹ D. Stamopoulos, N. Moutis, M. Pissas, and D. Niarchos, *Phys. Rev. B* 72, 212514 (2005).
- ³² M. G. Flokstra, N. Satchell, J. Kim, G. Burnell, P. J. Curran, S. J. Bending, J. F. K. Cooper, C. J. Kinane, S. Langridge, A. Isidori, N. Pugach, M. Eschrig, H. Luetkens, A. Suter, T. Prokscha, and S. L. Lee, *Nat. Phys.* 12, 57 (2016).
- ³³ G. A. Ovsyannikov, V. V. Demidov, Yu. N. Khaydukov, L. Mustafa, K. Y. Constantinian, A. V. Kalabukhov, and D. Winkler, *J. Exp. Theor. Phys.* 122, 738 (2016).
- ³⁴ P. G. de Gennes, *Superconductivity of Metals and Alloys*, Benjamin, New York, 1966 (Chap.5).
- ³⁵ J. B. Ketterson and S. N. Song, *Superconductivity*, Cambridge University Press, 1999 (Part III).
- ³⁶ Klaus Halterman and Oriol T. Valls, *Phys. Rev. B* 65, 014509 (2001); Klaus Halterman, Oriol T. Valls, and Paul H. Barsic, *Phys. Rev. B* 77, 174511 (2008).
- ³⁷ Hao Meng, Lin Wen, Guo-Qiao Zha, and Shi-Ping Zhou, *Phys. Rev. B* 83, 214506 (2011).
- ³⁸ L. D. Landau, E.M. Lifshitz, *Quantum Mechanics, Non-Relativistic Theory* (third ed.) Pergamon, Elmsford, NY (1977).
- ³⁹ Hao Meng, Xiuqiang Wu and Zhiming Zheng, *Europhys. Lett.* 104, 37003 (2013).
- ⁴⁰ A. A. Abrikosov, L. P. Gor'kov, *Sov. Phys. JETP* 15, 752 (1962).
- ⁴¹ F. S. Bergeret, A. F. Volkov and K. B. Efetov, *Europhys. Lett.* 66, 111 (2004).